Conceptual and laboratory exercise to apply Newton's second law to a system of many forces

Carl E Mungan

Physics Department, US Naval Academy Annapolis, MD 21402-1363, USA

E-mail: mungan@usna.edu

Abstract

A pair of objects on an inclined plane are connected together by a string. The upper object is then connected to a fixed post via a spring. The situation is first analysed as a classroom exercise in using free-body diagrams to solve Newton's second law for a system of objects upon which many different kinds of force are acting (string tension, spring force, gravity, normal force, and friction). Next, the setup is replicated in the laboratory using rolling carts with attached force sensors (to measure the string and spring forces) and a motion detector (to measure the position, velocity and acceleration of the objects). After characterizing the rolling friction, cart masses, incline angle and spring constant, the kinematics and dynamics of the system can be accurately modelled with no free parameters. Representing the data in different ways, notably plotting quantities as a function of the displacement of the carts instead of elapsed time, greatly assists in their interpretation. For example, the acceleration of the carts lies along two straight lines when plotted in that way, the mechanical energy has a zigzag shape and the velocity of the carts traces out a set of joining half-ellipses in phase space.

Introduction

In lectures in introductory physics, students are introduced one by one to a variety of forces, including gravity, normal force, friction, tension in a string and spring force. Simple models for reasoning about and making calculations with these forces are presented. The importance of free-body diagrams (FBDs) for linking these forces to the kinematics describing the motion of an object is emphasized by instructors, and yet most students see the construction of such diagrams as an unnecessary extra burden. Often they instead tackle problems simply by finding a solved example in their textbook and making minor changes to the resulting formulae to adapt it to their situation. An FBD does not appear to them to be a useful tool for problem solving because they can often guess what to plug into the left-hand side of $\mathbf{F} = m\mathbf{a}$ when few forces act on an object. To show the true utility of an FBD, it is necessary for students to work on exercises where a rich combination of forces acts simultaneously. Such a situation is presented in this article.

Considering next the laboratory portion of the introductory course, students typically perform experiments that individually treat horizontal kinematics, inclined planes, oscillatory motion, Atwood-type setups and at least some aspects

0031-9120/12/030274+14$33.00

Report Documentation Page

Form Approved
OMB No. 0704-0188

1. REPORT DATE **2012**	2. REPORT TYPE	3. DATES COVERED **00-00-2012 to 00-00-2012**

4. TITLE AND SUBTITLE **Conceptual and laboratory exercise to apply Newton's second law to a system of many forces**	5a. CONTRACT NUMBER 5b. GRANT NUMBER 5c. PROGRAM ELEMENT NUMBER
6. AUTHOR(S)	5d. PROJECT NUMBER 5e. TASK NUMBER 5f. WORK UNIT NUMBER
7. PERFORMING ORGANIZATION NAME(S) AND ADDRESS(ES) **US Naval Academy,Physics Department,Annapolis,MD,21402-1363**	8. PERFORMING ORGANIZATION REPORT NUMBER
9. SPONSORING/MONITORING AGENCY NAME(S) AND ADDRESS(ES)	10. SPONSOR/MONITOR'S ACRONYM(S) 11. SPONSOR/MONITOR'S REPORT NUMBER(S)

12. DISTRIBUTION/AVAILABILITY STATEMENT

Approved for public release; distribution unlimited

13. SUPPLEMENTARY NOTES

14. ABSTRACT

A pair of objects on an inclined plane are connected together by a string. The upper object is then connected to a fixed post via a spring. The situation is first analysed as a classroom exercise in using free-body diagrams to solve Newton?s second law for a system of objects upon which many different kinds of force are acting (string tension, spring force, gravity, normal force and friction). Next, the setup is replicated in the laboratory using rolling carts with attached force sensors (to measure the string and spring forces) and a motion detector (to measure the position, velocity and acceleration of the objects). After characterizing the rolling friction, cart masses, incline angle and spring constant, the kinematics and dynamics of the system can be accurately modelled with no free parameters. Representing the data in different ways, notably plotting quantities as a function of the displacement of the carts instead of elapsed time, greatly assists in their interpretation. For example, the acceleration of the carts lies along two straight lines when plotted in that way, the mechanical energy has a zigzag shape and the velocity of the carts traces out a set of joining half-ellipses in phase space.

15. SUBJECT TERMS

16. SECURITY CLASSIFICATION OF:			17. LIMITATION OF ABSTRACT	18. NUMBER OF PAGES	19a. NAME OF RESPONSIBLE PERSON
a. REPORT **unclassified**	b. ABSTRACT **unclassified**	c. THIS PAGE **unclassified**	**Same as Report (SAR)**	**14**	

Standard Form 298 (Rev. 8-98)
Prescribed by ANSI Std Z39-18

of retarding forces (static and sliding friction, and perhaps simple speed-dependent drag forces) using motion detectors and force sensors. This variety of experiments affords the opportunity for a summative laboratory experience in which all of these ideas are combined in a single experimental setup. To maximize its pedagogical benefits, this capstone laboratory is here integrated with the conceptual exercise of Newton's second law described in the preceding paragraph. It is particularly satisfying that no free parameters are needed to model the experimental results. By this stage of the course, students have built up their understanding of the concepts to the point that they can successfully account for all observable effects. Physics really does work!

At least two other side benefits of the laboratory exercise described in this article also accrue to students. First, it is a convincing example of the power of alternative representations in understanding data. Used in their conventional manners, motion detectors and force sensors respectively measure kinematic quantities and forces as functions of time. It will turn out here that it is much more useful to instead plot them as functions of position. Further insights can be obtained from phase-space plots and from energy diagrams. Secondly, the laboratory work presents a special opportunity to help students to develop a richer understanding of frictional effects. In particular, the concept of rolling friction, important in many real-world devices but often neglected in the physics curriculum, plays a critical role here.

The article is organized into two major sections, geared to an Advanced Placement or A-level physics course in a secondary school or introductory college course. The first section is the core material, while the additional theory and analysis presented in the second section are mainly for enrichment and further exploration.

The free-body diagrams and experiment

Two objects are investigated that are simultaneously subject to a variety of forces. The goals of the study are to improve students' conceptual understanding of how to solve Newton's second law for a reasonably complex situation and to enrich their physical intuition by then examining a similar setup in the laboratory.

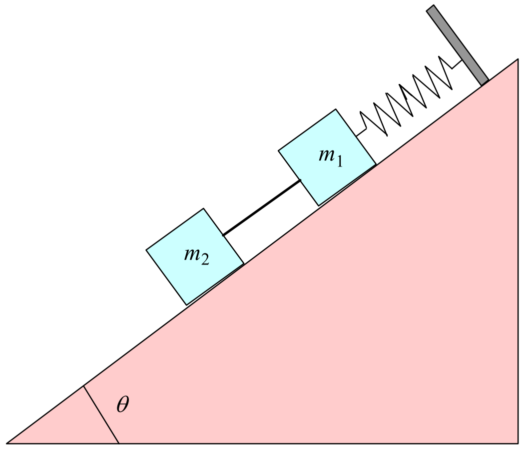

Figure 1. Sketch of the setup for the classroom exercise.

Classroom exercise

Begin with the following problem that groups of 2–3 students should work on together. It is assumed that the relevant individual forces have already been discussed previously in the course and that the students have some experience with constructing FBDs. In my own classes, I require that FBDs include arrows (carefully distinguished from the force arrows) labelled a and v (or the notations '$a = 0$' and '$v = 0$' if appropriate) and x and y to denote the positive directions of acceleration, velocity and the coordinate axes for each object of interest. The known directions for these four quantities should be used if they are given or implied in a problem; otherwise, any reasonable choice can be adopted. As will be apparent below, omitting these arrows on an FBD makes it much harder to successfully 'translate' the diagram into equations describing the components of Newton's second law.

Two blocks are connected by a string and are sliding on a plane inclined at angle θ relative to the horizontal, as drawn in figure 1. The coefficient of kinetic friction between either block and the plane is μ_k. The upper block has mass m_1 and is connected to a fixed post by a spring of stiffness constant k. The lower block has mass m_2. The blocks are released from rest with the spring at its relaxed length (i.e. the length it has before attaching the blocks to its lower end). Draw FBDs of each block at some instant in time when the spring has stretched a distance d, assuming that both blocks are in motion at that instant. Then use your FBDs to find an expression for the tension in the string connecting the two blocks at that instant (expressed in terms of givens and known constants, possibly including θ, μ_k, m_1, m_2, g, k and d).

The usual idealizations about the forces can be assumed:

- the string is massless and cannot stretch;
- the spring is massless and obeys Hooke's law;
- the frictional force on a block equals μ_k multiplied by the normal force of the plane on the block.

However, rather than reminding students about these concepts in a pronouncement from the front of the room, it would be better to let groups discuss ideas among themselves. The instructor can circulate around the room, giving help to groups that want it.

Evidently the blocks are going to oscillate up and down the incline, and eventually come to rest somewhere below their starting points. The FBDs are snapshots of the blocks at some instant of their motion. Students need to realize that the details of the FBDs depend on whether the blocks are moving up or down the plane at the instant of interest. So after some time of group work, a class discussion should be held in which the various relevant forces should be listed (by name) on the board, together with anything that can be said about their magnitudes and directions. The class may eventually wish to agree on a particular direction for the velocities of the blocks, for the sake of definiteness. They can then return to their groups to continue the exercise.

Here is a polished solution. Choose a coordinate system with x pointing down the incline parallel to its surface and y pointing perpendicularly away from the incline. Assuming that the blocks are sliding down the incline, figures 2(a) and (b) are FBDs for blocks 2 and 1, respectively. In the y directions, the force components must balance since the blocks can only accelerate parallel to the surface of the incline. Thus

$$N_1 = m_1 g \cos\theta \Rightarrow f_1 \equiv \mu_k N_1 = \mu_k m_1 g \cos\theta \tag{1a}$$

and similarly

$$N_2 = m_2 g \cos\theta \Rightarrow f_2 \equiv \mu_k N_2 = \mu_k m_2 g \cos\theta. \tag{1b}$$

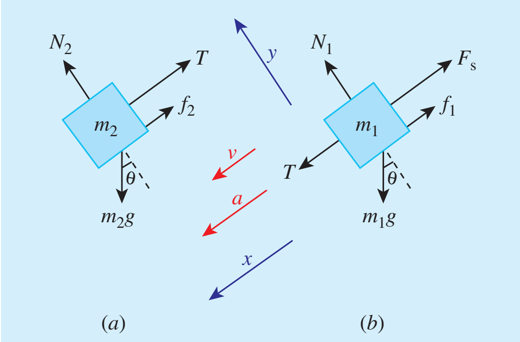

Figure 2. Both blocks have the same acceleration a and speed v and are acted upon by the same tension T since they are connected by an ideal string. The same coordinate system is chosen for both blocks. The normal forces are indicated by N, the frictional forces by f and the gravitational forces by mg with subscripts 1 and 2 for the two blocks. The spring force on block 1 is F_s. It is assumed that v and a point down the incline for specificity.

Noting that the magnitude of the spring force is given by $F_s = kd$ at the instant of interest, the x-component of Newton's second law can be written for block 1 as

$$T + m_1 g \sin\theta - \mu_k m_1 g \cos\theta - kd = m_1 a_x \tag{2a}$$

and for block 2 as

$$m_2 g \sin\theta - T - \mu_k m_2 g \cos\theta = m_2 a_x. \tag{2b}$$

Note that a must bear the subscript x. Without the subscript, a denotes the magnitude of the acceleration vector **a** and therefore cannot be negative. With the subscript, a_x is the x-component of **a** and can have either sign [1]. It is again worth interrupting the groups to have a class discussion about the signs of the x-components of the velocity and acceleration. Downhill sliding of the blocks means that $v_x > 0$ but not necessarily that $a_x > 0$. The sign of a_x depends on whether the blocks are speeding up or slowing down as they progress down the incline. Without getting into all the details of the stretch of the spring and the role of friction, it is intuitively clear that the blocks will be speeding up when they are high up the incline (e.g. just after release) and slowing down when they are far down the incline (i.e. about to turn around and start climbing back up it).

Based on this class discussion of a_x, it should be apparent that there are some subtleties involved with it and hence further study of the acceleration is deferred to the laboratory. The present classroom exercise only asks students to find an expression for the tension T when the spring is stretched by d. The key insight for this purpose is that equations (2a) and (2b) are two equations in two unknowns (a_x and T) and thus can be solved simultaneously by any of several methods, giving groups the opportunity to exercise some creativity. One way to do so is to divide the left-hand side of equation (2a) by m_1 and the left-hand side of equation (2b) by m_2 and equate them to eliminate a_x. Solving the result for T then gives

$$T = \frac{m_2}{m_1 + m_2} kd. \tag{3}$$

This final expression for T is simple and concrete. It might be worthwhile to check it by showing that it has the correct units and that it reduces to the expected result for cases such as $m_1 = 0$, $m_2 = 0$ and $m_1 = m_2$. At first sight, it seems remarkable that equation (3) is independent of θ. Intuitively one might have expected the tension to increase with increasing tilt of the track. But keep two points in mind. First, it is the spring that ultimately drives the motion: equation (3) shows that the tension T is directly proportional to the spring force kd. Second, equation (3) only applies if θ is larger than the value $\theta_{\min} = \tan^{-1} \mu_s$, because the x-component of the gravitational force $m_{\text{tot}} g \sin\theta$ must exceed the static frictional force $\mu_s m_{\text{tot}} g \cos\theta$ with the blocks (of total mass $m_{\text{tot}} = m_1 + m_2$) in their initial position when the spring is unstretched, or otherwise they will never begin to move! Thus the tension actually does depend on θ in the sense that it is zero for $\theta \leqslant \theta_{\min}$ (even for an ideal frictionless system, some initial tilt of the track is thus required) and it only attains the value given by equation (3) after the blocks begin to move and any initial slackness in the string is removed.

In any case, the real goal of the exercise is not to obtain equation (3), but to draw the FBDs and properly use them to write down and work with Newton's second law. With that in mind, and in preparation for the follow-up experiment, it is more important that groups can confidently draw figure 2 and write down equations (2a) and (2b) than that they can simultaneously solve the latter two equations.

Laboratory preparation: acceleration as a function of spring stretch

So far, simple expressions for the spring force $F_s = kd$ and for the string tension $T = m_2 kd / m_{\text{tot}}$ have been found as a function of the stretch d of the spring from its relaxed position. Neither of these forces depends on the direction of the velocity or acceleration of the blocks, and they can be straightforwardly measured in the laboratory using a pair of force sensors and a motion detector, as described in 'Laboratory experiment: setup, characterization of parameters and data collection'. To add richness to the laboratory experience, the acceleration of the blocks can also be determined by the motion detector. Unlike F_s or T, when the acceleration is plotted versus d the data points are found to lie along two straight lines rather than a single one. The theory behind this result is described here. Instructors who prefer a 'discovery' approach in the laboratory may wish to withhold presenting this theory until after the measurements have been performed.

Anticipating the result, from now on I will subscript the acceleration a with 'down' or 'up', depending on whether the blocks are sliding down or up the incline, respectively. Let us start with the case of downhill sliding, as treated in 'Classroom exercise'. The x-component of the acceleration can be found by adding equations (2a) and (2b) together to eliminate T. Rearranging then leads to

$$a_{\text{down},\,x} = g(\sin\theta - \mu_k \cos\theta) - kd/(m_1 + m_2). \tag{4}$$

We see that $a_{\text{down},\,x}$ is positive only if d is less than some critical value d_c given by setting the right-hand side of equation (4) to zero,

$$d_{\text{down,c}} = \frac{(m_1 + m_2) g \cos\theta}{k} (\tan\theta - \mu_k). \tag{5}$$

As a technical aside, which is probably worth mentioning in class only if some student explicitly asks about it, $d_{\text{down,c}}$ is necessarily positive because $\tan\theta > \mu_s \geqslant \mu_k$. It must be the case that $\tan\theta > \mu_s$ if the blocks are to begin moving after they are released from their initial positions, as mentioned in 'Classroom exercise'. Furthermore, the static and kinetic coefficients of friction must physically satisfy the relation $\mu_s \geqslant \mu_k$. Otherwise a block placed at rest on an incline with angle θ given by $\tan^{-1} \mu_s < \theta < \tan^{-1} \mu_k$ could neither slide nor stay at rest!

It is left as an exercise for the reader (or their students) to repeat the preceding analysis for the situation when the blocks slide up the incline. The FBDs in figure 2 remain the same except that we must reverse the three arrows for the directions of v, f_1 and f_2. Equations (1*a*) and (1*b*) remain unchanged, but in each of equations (2*a*) and (2*b*) one must change the sign in front of μ_k. Replacing a_x with $a_{up,x}$, equations (4) and (5) then become

$$a_{up,x} = g(\sin\theta + \mu_k \cos\theta) - kd/(m_1 + m_2) \quad (6)$$

and

$$d_{up,c} = \frac{(m_1 + m_2)g\cos\theta}{k}(\tan\theta + \mu_k). \quad (7)$$

Comparing equations (4) and (6), one sees that the acceleration of the blocks when plotted against d is predicted to describe two straight lines with equal (negative) slopes but different intercepts, one for upward and the other for downward velocities along the incline. In 'Laboratory experiment: setup, characterization of parameters and data collection', this prediction is quantitatively verified in the laboratory.

Laboratory experiment: setup, characterization of parameters and data collection

An attempt was made to reproduce the setup in figure 1 with standard equipment available in an introductory physics laboratory. However, even when relatively smooth blocks and incline were used, kinetic friction was found to rapidly damp out the motion and to occasionally cause the blocks to veer sideways rather than remaining on a strictly linear trajectory up and down the ramp. In order to ensure smooth one-dimensional motion lasting at least a minute (for manageable incline angles), the blocks were replaced with rolling carts on a grooved aluminum track. This replacement means that the sliding friction becomes rolling friction, and consequently the coefficient of kinetic friction μ_k will from now on be replaced by the coefficient of rolling friction μ. A careful treatment of the theory of rolling friction [2] shows that one can model the friction by the same form used in equations (1), namely $f = \mu N$. Therefore it is not important that students understand the details of rolling friction to conduct and interpret the present experiment. In fact, at least two articles [3, 4] that use the same apparatus as is used here do not even bother to change the name or subscript of the frictional force, but continue to call it kinetic friction with coefficient μ_k. It would be preferable to at least alert students to the idea of rolling friction, but from the point of view of modelling the experimental results it actually makes no difference.

The list of equipment for the present experiment using rolling carts is given in the accompanying sidebar, for the benefit of instructors who wish to replicate it in their schools. For specificity, PASCO model numbers are given for some of the key apparatus, but similar equipment from Vernier, PHYWE or other vendors can also be used.

There are two sets of procedures that students need to follow to obtain data that can be fully compared to the theory presented in 'Laboratory preparation: acceleration as a function of spring stretch' with no free parameters. Most of these experimental steps are relatively standard procedures that students should be familiar with from previous laboratory work in the course. Thus instructors can choose how detailed to make the instructions they give to the laboratory groups, ranging from a detailed recipe to only a general discussion of the available equipment and goals.

The first set of procedures consists in quantitatively characterizing the experimental parameters. In brief, we need the values of θ, μ, m_1, m_2, g, k and the equilibrium stretch s of the spring (beyond its relaxed length) with the carts attached and at rest. The value of g can either be assumed to be 9.8 m s^{-2} (which is what I did and which is a reasonable value at the latitude of my school), or a value can be determined from the standard geodetic formula or from any independent experimental method of choice.

Attach force sensors to the top of each cart. Label them '1' and '2' in pencil to keep track of which is which. Weigh them to determine m_1 and m_2. I found $m_1 = m_2 \equiv m = 0.8319 \pm 0.0006$ kg since I used identical carts and force sensors. (An accurate electronic scale was used to measure the masses. All other quantities reported in this article were obtained from fits or from visually inspecting lengths using a metre stick and consequently have precisions of only 1–3%, with correspondingly fewer reported significant figures.)

Calibrate the stiffness constant k by attaching one end of the spring to a vertical hook and freely

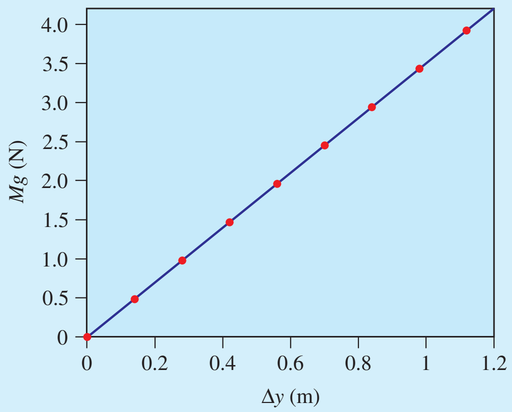

Figure 3. Experimental measurements (red dots) to determine the spring constant k from a linear fit (blue line).

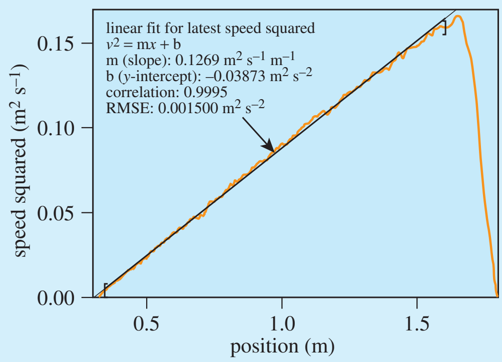

Figure 4. Experimental measurements (orange line) to determine the coefficient of friction μ from a linear fit (black line).

hanging known weights Mg from the other end. Use a metre stick to measure the resulting changes in length of the spring, Δy. Use a sufficient variety of weights that the stretch of the spring spans the range of distances that it will undergo on the track in the actual experiment. I found that hanging from 50 to 500 g masses in 50 g increments worked well. A graph of the resulting values of Mg versus Δy is presented in figure 3. A linear fit gives a slope of $k = 3.5 \pm 0.1$ N m^{-1}.

Afterwards, the relaxed spring will probably be permanently slightly elongated in length, with adjacent coils no longer touching each other. Measure that relaxed length s_i, which in my case was 12 cm. We will use this value later to determine s.

Next the coefficient of friction is measured. Level the track and clip a motion detector to its end. Choose either of the carts and arrange the attached force sensor's electric cable on top of it so that it is out of the way. Starting from the far end of the track, give the cart a push towards the motion detector and collect data on its position. Catch the cart before it hits the motion detector. Plot the speed squared v^2 versus the position x of the cart. (One easy way to do this within LoggerPro is to insert a manually calculated column into the data table equal to velocity multiplied by velocity.) Fit a straight line to the portion of the data while the cart is smoothly in motion. Divide the resulting slope by $2g$ to find the value of μ. The theory behind this procedure is simple. The work–kinetic-energy theorem implies that

$$\tfrac{1}{2}mv^2 - \tfrac{1}{2}mv_0^2 = -\mu mg\Delta x \qquad (8)$$

where Δx is the (positive) distance moved by the cart starting from its initial position x_0 (when it has speed v_0). Thus $\Delta x = x_0 - x$ because the cart is moving towards the motion detector so that $x < x_0$. Hence a graph of v^2 versus x has a positive slope of $2g\mu$. The result is independent of the mass m of the cart and thus should apply to either cart, assuming that both have the same construction (and neither has been mistreated), but it only takes a few extra minutes to roll the other cart on the track and recollect the data to make sure that both carts give the same slope.

Figure 4 presents typical data for a low initial speed of a cart, with the analysis performed directly in LoggerPro. The slope implies $\mu = 0.0065 \pm 0.0002$. The same slope was found for high initial speeds of the cart (up to at least 0.7 m s^{-1}), proving that the coefficient of rolling friction is independent of speed, as was implicitly assumed to be the case in deriving equations (4) and (6). This result concludes the characterization of the experimental parameters.

The second set of procedures is to set up the track and carts as depicted in the photograph in figure 5, and to collect kinematic and dynamic data using them. Notice the considerable stretch of the spring from its relaxed length of $s_i = 12$ cm. With the two carts attached and at rest, the loaded length of the spring was found to be $s_f = 90$ cm. Therefore its equilibrium stretch is $s \equiv s_f - s_i = 78 \pm 1$ cm. This number is used to convert values

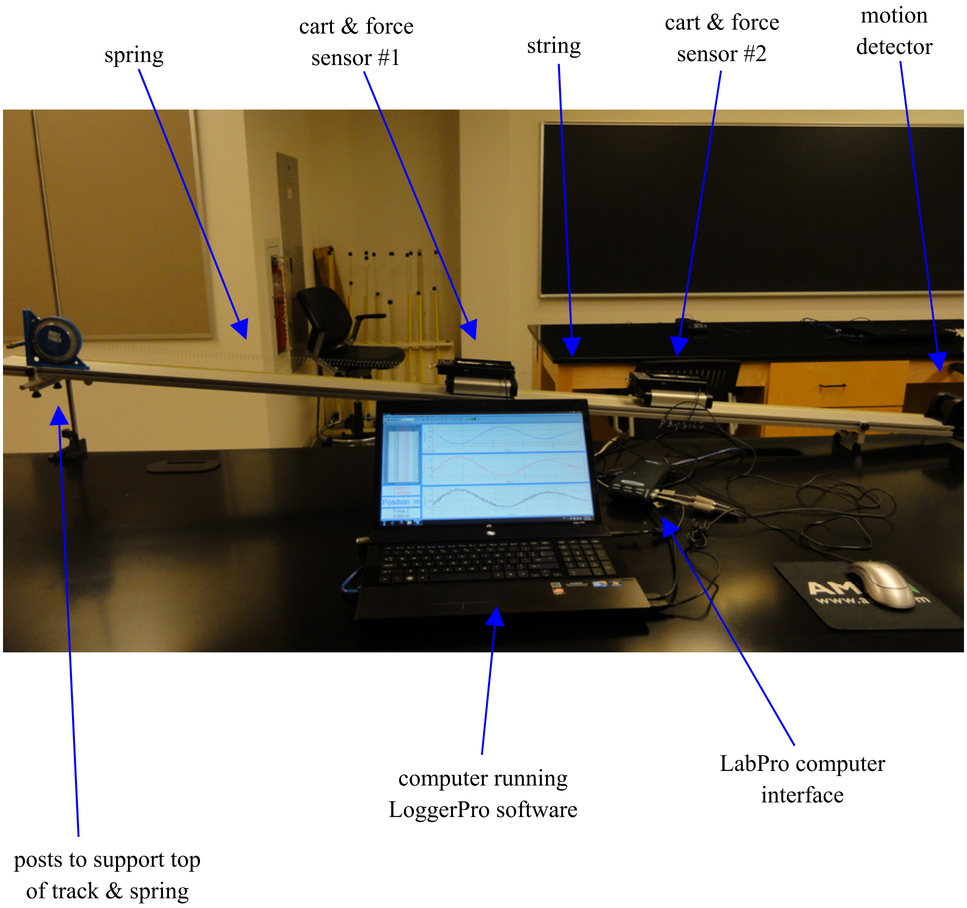

Figure 5. Experimental setup for measuring the forces on and kinematics of two rolling carts.

of position x measured by the motion detector at the bottom of the track into stretches d of the spring. The angle finder at the top of the track was used to set the inclination at approximately 10° above the horizontal. But a more accurate value of $\theta = 9.7° \pm 0.1°$ was computed from the inverse tangent of a 37.5 cm rise of the track measured over a 218.5 cm run using a metre stick.

LoggerPro was set up to collect three graphs as a function of time: force sensor #1 (measuring the spring force F_s), force sensor #2 (measuring the string tension T), and the motion detector (measuring position x, velocity v or acceleration a of the lower end of cart #2). The data collection was adjusted to measure 40 samples per second for 15 s. To reduce the noise, the number of points for derivative and smoothing calculations was chosen to be 29. The two force sensors were individually calibrated by hanging 500 g from their hooks vertically. They were zeroed by placing them on the track in their correct orientations with nothing attached to their hooks.

The spring and string were then attached to the carts. (The electric cables running from the LabPro interface to the two force sensors were arranged so that they did not snag on any obstacles during the oscillations of the carts.) One end of the spring ran to a horizontal post at the top of the track and the other end ran to the hook on force sensor #1. One end of the string was tied to the back of force sensor #1 and the other end ran to the hook on force sensor #2. The spring and string were centred both horizontally and parallel to the track. The motion detector was clipped onto the bottom end of the track. It was then zeroed with the carts at rest. It therefore follows that the stretch of the spring is equal to $d = s - x$, with x oscillating about zero as can be seen in the typical

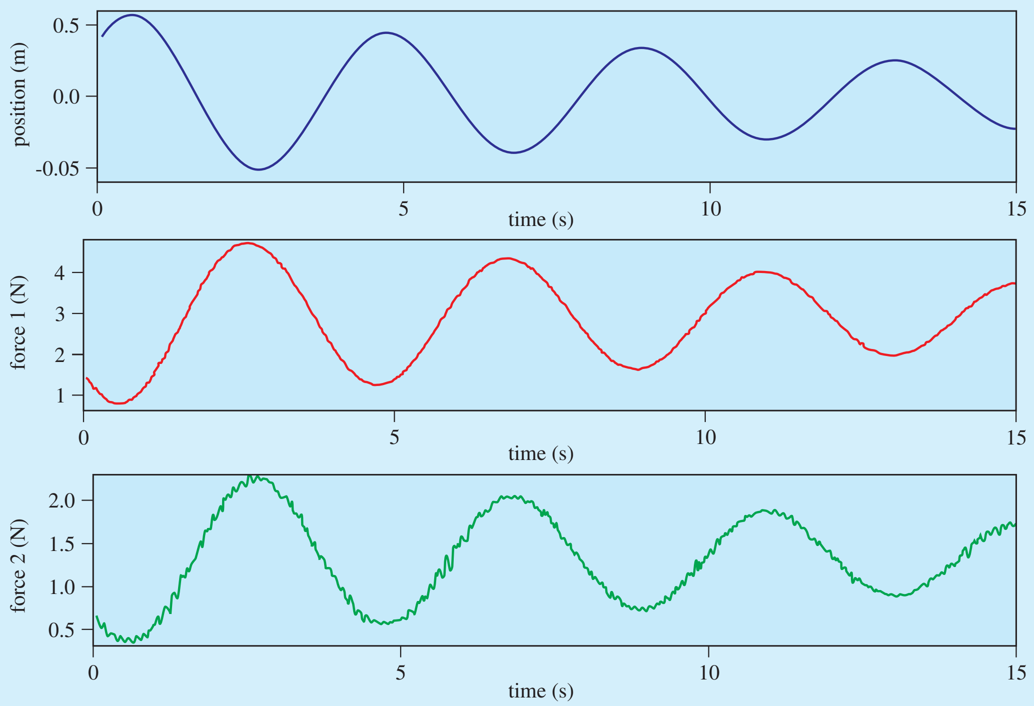

Figure 6. Typical data run in LoggerPro indicating graphs of properly calibrated and zeroed values of x, F_s and T (from top to bottom) over a 15 s interval.

data run shown in figure 6. To collect these data, cart #2 was pulled down the track to within about 15 cm from the motion detector and released. Then the collect button was clicked. Note from the top graph in figure 6 that data collection started after the carts had already climbed most of the way up the incline, thereby eliminating any distracting initial features due to the start of motion. Also the measurements stop while there is still enough motion of the carts that the data have not become overly noisy.

The position graph (top pane in figure 6) has the shape expected for damped sinusoidal motion. However, instructors should not jump to the conclusion that the detailed functional form of this curve is

$$x(t) = Ae^{-\gamma t}\cos(\omega' t + \phi), \quad \text{[WRONG!]} \quad (9)$$

where $\gamma \equiv b/2m_{\text{tot}}$ and $\omega' = (k/m_{\text{tot}} - \gamma^2)^{1/2}$, appropriate to simple harmonic oscillations of an object of total mass $m_{\text{tot}} \equiv m_1 + m_2$ in the presence of a resistive (drag) force $-bv$ that is linearly proportional to the speed of motion [5]. In our case, the resistive (rolling frictional) force is independent of the speed of motion and hence a different expression for $x(t)$ results [6], as is discussed in 'Laboratory results: basic analysis of the kinematics and dynamics'.

The two forces plotted in the lower panels of figure 6 are proportional to d and hence to x. Since the acceleration equals the second derivative of the position x which is sinusoidal, it follows that the force graphs are phase shifted by 180° relative to the position graph, i.e., troughs of the top graph coincide with crests of the other two graphs and vice versa. A student can quickly change the top graph within LoggerPro into a plot of acceleration (rather than position) versus time, and then all three graphs will have the same phase. The larger levels of noise seen in the bottom compared to the middle graph probably originate both from the expanded vertical scale, noting that equation (3) predicts that T should be equal to half of F_s since $m_1 = m_2$, and from vibrations in the wheels of cart #1 to which the string is attached.

The data collection can be repeated with slight variations in the release of the carts, time delay until the collect button is clicked, exact pointing of the motion detector and parameters in the software until one is satisfied with the results. They should then be saved to a file for the analysis detailed in 'Laboratory results: basic analysis of the kinematics and dynamics'. Although that analysis can be performed within LoggerPro itself, it is easier to use a graphing software package such as a spreadsheet.

Laboratory results: basic analysis of the kinematics and dynamics

So far, the data for the kinematics and forces have been plotted in LoggerPro as a function of time. But according to the theory presented in the previous subsections, it is easier to model the data if we replot them versus position instead of time. Since LoggerPro saves six columns of data by default (corresponding to t, $F_1 = F_s$, $F_2 = T$, x, v_x and a_x) it is easy to do this within a spreadsheet such as Excel by selecting the two desired columns of data. The results are plotted in figures 7(a)–(c) as the blue dots. The theoretical predictions are graphed by the solid lines, using the values of the parameters determined in 'Laboratory experiment: setup, characterization of parameters and data collection' (allowing them to vary at most within their specified precisions).

Figure 7(a) plots the spring force. Recalling that $d = s - x$, the model predicts that

$$F_s = k(s - x), \tag{10}$$

shown as the red line, in excellent agreement with the data. Panel (b) graphs the tension in the string connecting the two carts together. Equation (3) can be rewritten in terms of x as

$$T = \frac{m_2 k}{m_1 + m_2}(s - x), \tag{11}$$

which is shown as the red line and again describes the measurements well. Finally, figure 7(c) plots the acceleration of the carts as a function of their position. In striking contrast to the plots in panels (a) and (b), the acceleration data lie along two straight lines, rather than only one. These two lines correspond to motion of the carts up the incline (corresponding to the red curve) and down the incline (green curve), with turn-arounds occurring at extremal values of a (when $v = 0$). These two theory curves use the mean values of all of the measured parameters with no undetermined coefficients. Since the motion detector is located

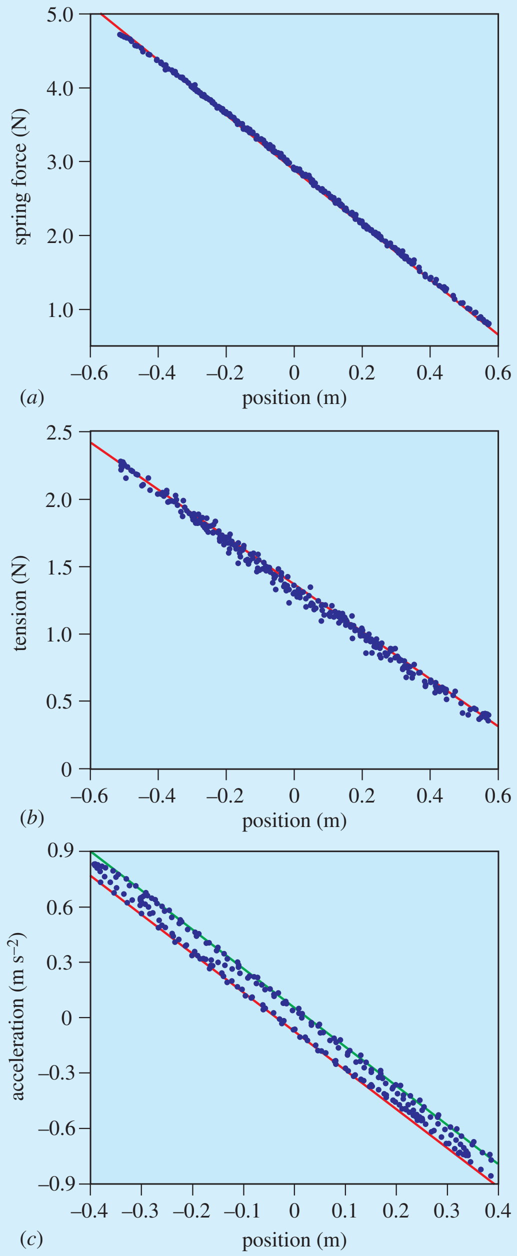

Figure 7. (*a*) Graph of the measured spring force F_s versus the position x of cart #2 (blue dots), together with a plot of the theoretical prediction (red line). (*b*) Graph of the measured tension T in the string versus the position x of cart #2 (blue dots), together with a plot of the theoretical prediction (red line). (*c*) Graph of the measured acceleration a_x of the carts versus the position x of cart #2 (blue dots), together with a plot of the theoretical prediction (red and green lines).

at the bottom of the incline, it measures $a_x > 0$ for accelerations directed up the incline, opposite to the convention of figure 2, and so we reverse the signs of equations (4) and (6) to obtain

$$a_{\text{down},\,x} = -g(\sin\theta - \mu\cos\theta) + k(s - x)/(m_1 + m_2) \quad (12)$$

for the green curve, and

$$a_{\text{up},\,x} = -g(\sin\theta + \mu\cos\theta) + k(s - x)/(m_1 + m_2) \quad (13)$$

for the red curve. The difference in the intercepts of these two curves is

$$a_{\text{down},\,x} - a_{\text{up},\,x} = 2g\mu\cos\theta \quad (14)$$

and thus the vertical separation between the two lines is a sensitive measure of rolling friction. The excellent fits demonstrate that μ is independent of θ and v, and that air drag is negligible (as further discussed in the appendix), at least for the range of motions investigated here.

Further analysis of the experimental data

So far the spring force F_s, the string tension T and the acceleration of the blocks a_x have been analysed as a function of position. One could stop here. However, there are additional interesting aspects of the data that can be mined from them, if time and student interest permit. Specifically, three other representations of the data will be discussed in this section.

Time dependence of the position

I have already argued that equation (9) is wrong because it only applies when the drag is linear in the speed of the object. In the present experiment, the frictional force is independent of the speed of the carts. It is not hard to conceptually deduce the correct expression for the resulting position of the carts as a function of time [7], although it requires a bit of care to write it down mathematically [8].

Consider some half-cycle of the motion of the carts, during which they are rolling down the incline. Throughout that interval of time (between successive zero-crossings of the velocity), the system of two carts (treated as a unit) is subject to only three force components along the incline: the spring force F_s, the x-component of the total weight $m_{\text{tot}}g$ of the two carts and the sum $f_{\text{tot}} = f_1 + f_2$ of the frictional forces on the carts. If the only force were F_s, then the carts would oscillate with constant amplitude A about the relaxed position $d = 0$ of the spring. Next imagine turning on gravity without friction. This situation corresponds to the familiar classroom discussion of a mass on a horizontal spring that is rotated until it is hanging vertically. The amplitude A of oscillation is unchanged; the only effect of turning on gravity is to shift the centre point of the oscillations to the new equilibrium position $d = s$. Finally, turn on the rolling friction. Since it is a constant force, its effect on the motion is analogous to gravity's effect (which is also a constant force). Namely the centre point of the oscillations is again shifted.

We can now mentally trace out the motion of the system. Start with the carts momentarily at rest near the top of the incline at $d = 0$ for the first half-cycle of the motion; that position is a 'top turning point.' The carts will begin to roll downhill. Eventually they will pass through the centre point of their downward motion, at which position the sum of the three force components along the incline is zero. At that centre point, $d = d_{\text{down,c}}$ as given by equation (5), with the kinetic coefficient μ_k replaced with the rolling coefficient of friction μ. The difference in position between a turning point and the equilibrium point defines the amplitude of motion. Consequently the amplitude of the carts' motion for the first half-cycle is $A_1 = d_{\text{down,c}}$. The carts will continue to roll downhill until they reach a 'bottom turning point' at a total spring stretch of double the amplitude, $d = 2A_1 = 2d_{\text{down,c}}$.

Next the carts will start rolling back uphill. But when that happens, the frictional force reverses direction. Consequently the spring position at which the three force components sum to zero changes to $d = d_{\text{up,c}}$ given by equation (7). The amplitude for this second half-cycle is the difference in position between the bottom turning point and this new equilibrium point, so that $A_2 = 2d_{\text{down,c}} - d_{\text{up,c}}$. The amplitude is thus decreased by $\Delta A \equiv A_1 - A_2 = 2m_{\text{tot}}g\mu\cos\theta/k$. This trend continues: the amplitude drops linearly (not exponentially) by ΔA every half-cycle until the carts come to rest at one of the turning points after a finite number of oscillations [9]. In further contrast to the viscous (speed-dependent) damping of equation (9), the angular frequency of oscillation is always equal to the undamped value of $\omega = \sqrt{k/m_{\text{tot}}}$.

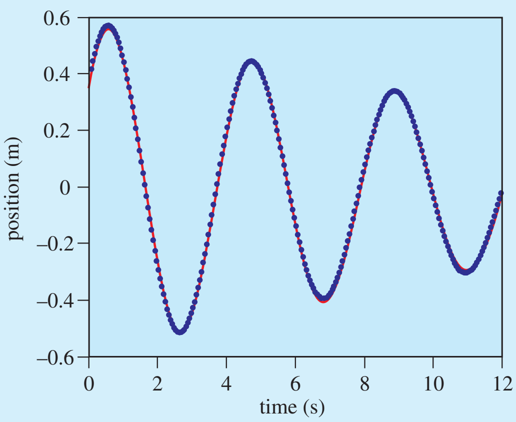

Figure 8. Graph of the measured position x of cart #2 (blue dots), together with a plot of the theoretical prediction (red curve).

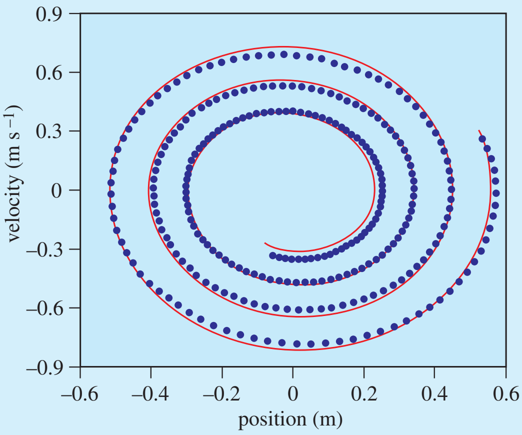

Figure 9. Phase-space plot of the velocity of the carts versus the position x of cart #2 (blue dots), together with the theoretical prediction (red curve).

Putting these ideas together, the amplitude in the nth half-cycle has the constant value

$$A_n = A_1 - (n-1)\Delta A = \frac{m_{\text{tot}} g}{k} \times [\sin\theta + \mu(1-2n)\cos\theta]. \tag{15}$$

Assuming one starts the measurement of time t with the spring at its relaxed length (i.e., $d = 0$ at $t = 0$), then n is calculated by dividing t by $T/2 = \pi/\omega$ and rounding upward to the next largest integer. The computed position of the carts as a function of time is given by

$$x(t) = A_n \cos(\omega t). \tag{16}$$

To compare this prediction to the experimental data graphed in the top panel of figure 6, we need to shift the origin of time t horizontally to account for the fact that $t = 0$ actually indicates when the collect button was clicked. The resulting curve is plotted in red in figure 8 and is in excellent agreement with the data points in blue.

Phase-space motion of the carts

Now that we have an accurate model for the position of the carts, we can differentiate equation (16) with respect to time to get the velocity of the carts,

$$v_x(t) = -A_n \omega \sin(\omega t), \tag{17}$$

where again t is actually calculated as $t - t_0$ with t_0 being the time the carts would be at rest at the unstretched position of the spring (by extrapolating backward in time). In practice, t_0 is found by shifting the calculated curve in figure 8 horizontally until it best coincides with the experimental data. To be accurate, the carts should be released from rest with the spring relaxed, to ensure that the amplitude of motion matches equation (15), rather than being released near the bottom of the incline as was done in the experimental procedures described in 'Laboratory experiment: setup, characterization of parameters and data collection'.

A graph of velocity versus position maps out what is known as a phase-space orbit. Any given point on such a curve specifies the initial conditions needed to uniquely determine the motion of the object thereafter. (In general, a solution of Newton's second law requires specification of x_0 and v_0.) In the presence of damping (without a compensating driving force), the orbit will gradually decay towards a point of zero velocity at some specific final position, without ever crossing itself. Consequently, for real undriven oscillators the phase-space trajectory is a clockwise inward spiral [10, 11]. Our experimental and predicted curves are plotted in figure 9 and show that behaviour, starting from a point of large positive position and small positive velocity near the right-hand edge of the figure.

If one has gone to the work of generating this visually appealing phase-space graph in class, it may make sense to follow up by discussing with students the actual mathematical shape of this orbit. During any half-cycle (between successive crossings of the horizontal central axis in figure 9 when $v = 0$) the amplitude of oscillation is a constant, just as it is for an undamped simple harmonic oscillator. But for an undamped oscillator, the phase-space trajectories are ellipses [11]. Consequently, each half-cycle of the graph in figure 9 is half of an ellipse, $(x/A_n)^2 + (v_x/A_n\omega)^2 = 1$ from equations (16) and (17). At the nth turning point, the semi-major and semi-minor axis lengths of a given ellipse suddenly decrease by a factor of $\Delta A/A_n$ according to equations (16) and (17), but the centre of the ellipse also shifts horizontally so that there is no discontinuity in the orbit.

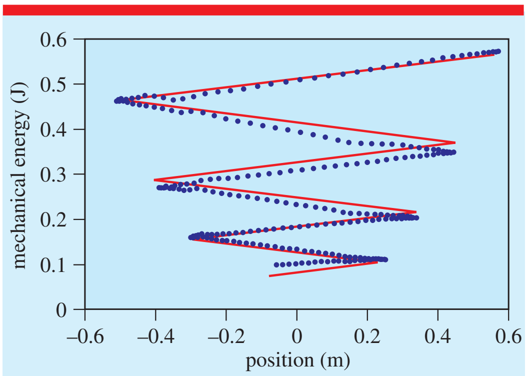

Figure 10. Graph of the mechanical energy of the system versus the position x of cart #2 (blue dots), together with the theoretical prediction (red curve).

Mechanical energy of the system

It is often instructive in studying oscillators to consider the kinds of energy involved [12]. In the present situation, there is kinetic energy of the two carts, elastic potential energy of the spring, gravitational potential energy as the carts move along the incline and thermal energy generated by rolling friction (as the wheels flex against the track and the bearings rub against the axles). The elastic potential energy is equal to

$$U_s = \tfrac{1}{2}kd^2 = \tfrac{1}{2}k(s-x)^2 \qquad (18)$$

and the gravitational potential energy is

$$U_g = m_{tot}gh \qquad (19)$$

where h is the height of the centre of mass of the two carts above some reference level. The simplest choice is to measure up from the table to the bottom of cart #2, since that is what the motion sensor monitors, so that $h = x\sin\theta$. Substitute that expression into equation (19) and then replace $m_{tot}g\sin\theta$ with ks, which must be equal to it because forces along the incline balance at the equilibrium position of the loaded spring. Now add together the two forms of potential energy to get a total of

$$U = \tfrac{1}{2}kx^2 \qquad (20)$$

after discarding an unimportant constant of $\frac{1}{2}ks^2$ (which can be eliminated by shifting the reference level appropriately). Equation (20) simply states the familiar fact that the total potential energy of the system is proportional to the square of the displacement x from the equilibrium (rather than the relaxed) position of the spring. The total kinetic energy of the system is

$$K = \tfrac{1}{2}m_{tot}v^2 \qquad (21)$$

and adding equations (20) and (21) gives the total mechanical energy $E = K + U$. Experimental values of E can be computed from the measurements of x and v by the motion sensor and our characterization of the masses and spring constant. The result is plotted versus position x as the blue dots in figure 10 and has a zigzag shape.

Theoretically it is easy to see how this shape arises. The analogue of equation (8) for the carts rolling on the incline is

$$\Delta E = -f_{tot}\Delta x = -\mu m_{tot}g\cos\theta\,\Delta x \qquad (22)$$

where f_{tot} is the sum of the rolling frictional forces on the two carts. Thus we predict that the energy drops linearly with a slope of magnitude $\mu m_{tot}g\cos\theta$ while x reverses direction each half-period of oscillation, as plotted in red in figure 10. Note that if we instead plotted E versus time t, the slope would not be constant and so the pattern would not simply be a straight line folded back on itself. Equation (22) compactly represents the conversion of mechanical energy into thermal energy by rolling friction.

Conclusions

Looking back over our journey in this article, we started by drawing free-body diagrams in figure 2 that are rich enough to challenge students who are used to skipping that step in solving Newton's second law. From figure 2, we found an expression for the tension that is simple and that turns out to be the same for both upward and downward motion of the blocks. It only depends on the mass ratio m_1/m_2 and on the spring force kd, and is independent of the individual masses of the blocks, the gravitational field, the angle of the incline and the coefficient of friction. On second thought, how can that be? In physics instruction, we often emphasize that solutions can be tested by considering limiting cases. But clearly the tension is not given by equation (3) in the limits that the angle of the incline becomes zero, the coefficient of friction becomes very large or in zero gravity. However, while T itself does not depend on θ, μ_k or g, its minimum value does for equation (3) to hold, in that we assume the blocks will begin to slide down the incline once released. This example serves as a caution against blindly taking limiting cases of a problem solution.

In contrast to the tension, we found that the acceleration of the blocks is different for uphill and downhill motions. To test this prediction, we went into the laboratory and employed carts instead of blocks, replacing the concept of sliding friction with rolling friction. Although the detailed mechanisms of these two kinds of friction are different, both can be modelled as a coefficient μ multiplied by the normal force N on the object. In particular, the rolling coefficient could be measured by pushing a cart along a level track, where the resulting slowing by friction is readily visible to students.

Although we were able to analyse the position of the carts (and hence their velocity and acceleration by differentiating) as a function of time in the form of equations (15) and (16), it required some care. Furthermore the graph in figure 8 does not immediately show the difference between motion up and down the track. For this purpose, it turned out to be much more revealing to plot the acceleration against position instead of time. Two straight lines then resulted, with the vertical spacing between them being directly proportional to the coefficient of rolling friction according to equation (14).

This technique of plotting quantities versus position also showed itself to be a useful way to interpret the variation in the spring force, string tension and mechanical energy of the system because each of them is then a straight line (folded over itself in the case of the energy). Another visually enlightening way to graph the motion of the system is in phase space. Each half-cycle of the motion in figure 9 turns out to describe half of an ellipse, whose major and minor axis lengths decrease by the same linear increment after each turning point.

The experiments and concepts presented here can be extended in other directions. Shaw [13] has shown that if a hanging weight drives the rolling of a solid cylinder, the frictional force can be in either the opposite or the same direction as the translational motion, depending on whether the string is wound around a disc whose radius is a small or a large fraction of the radius of the cylinder, respectively. Note that the rolling friction is negligible compared to the driving force in Shaw's experiment, and hence the friction he is measuring is static (in the absence of slipping) not rolling. Finally, getting closer to the extramural interests of many students, the free rolling (coasting) of vehicles (such as bicycles [14] or cars [15]) can be measured. Air drag becomes sizeable once the speed gets high enough (above 5–10 m s^{-1}), but at low speeds rolling friction dominates. The overall resistance depends on tyre inflation, transmission losses and streamlining of the shape [16].

Acknowledgments

I thank Midshipman Alexander Pybus in my General Physics I course, whose in-class analysis of figure 1 motivated this article. Thanks also go to Ensign James Kelly for discussions and measurements of the rolling friction, and to Professor Michael Faleski from Delta College who suggested plotting the mechanical energy.

Sidebar: Laboratory equipment list (per student station)

- two PASCO collision carts (ME-9454);
- two PASCO dual-range force sensors (used on the ±10 N scale);
- one PASCO 2.2 m track (ME-9779);
- one PASCO motion sensor (used on the narrow-beam setting);
- one PASCO harmonic spring (ME-9803);
- computer with LabPro interface and LoggerPro software;
- posts (to support the track and spring);

- 25 cm thread (to connect the two carts together);
- hanging weights (to calibrate the spring constant and force sensors);
- electronic scale (to weigh the carts with their attached force sensors, m_1 and m_2);
- angle finder (to adjust the track to $\theta \approx 10°$);
- metre stick (to measure the spring stretch and exact track angle).

Appendix. Air drag on the rolling carts

Here it is shown that air drag can be ignored for the speeds of this experiment. The rms speed of the carts during the 15 s interval in figure 6 is calculated from the data to be $\bar{v} = 0.40$ m s^{-1}. The cross section of a cart with its attached force sensor is roughly square with an area of approximately $A \approx 50$ cm^2. Consequently the Reynolds number is large enough that the air resistance is quadratic (rather than linear) in the speed, $F_D \approx \frac{1}{2}A\rho\bar{v}^2$, where $\rho = 1.2$ kg m^{-3} is the density of air [17]. We can compare this value to the coefficient of friction measured in figure 4 by dividing by the weight of the cart to get $F_D/mg = 6 \times 10^{-5}$. This value is only about 1% of the value of μ found experimentally. Therefore the air drag on the carts is on average 100 times weaker than the rolling friction and is consequently negligible.

Received 2 September 2011, in final form 23 September 2011
doi:10.1088/0031-9120/47/3/274

References

[1] Mungan C E 2010 Sign issues for one-dimensional vectors *Phys. Teach.* **48** 439–40
[2] Krasner S 1992 Why wheels work: a second version *Phys. Teach.* **30** 212–5
[3] Boyette T R and Haase D G 1996 An apparatus evaluation *Phys. Teach.* **34** 298–9
[4] Venable D D, Batra A P and Hubsch T 2001 Modifying the inclined-plane experiment *Phys. Teach.* **39** 215–7
[5] Halliday D, Resnick R and Walker J 2011 *Fundamentals of Physics* 9th edn (Hoboken, NJ: Wiley) p 400
[6] Molina M I 2004 Exponential versus linear amplitude decay in damped oscillators *Phys. Teach.* **42** 485–7
[7] Clark C B and Swartz C E 1996 Analytic solution for the oscillator with classical friction *Phys. Teach.* **34** 550–4
[8] Onorato P, Mascoli D and DeAmbrosis A 2010 Damped oscillations and equilibrium in a mass-spring system subject to sliding friction forces: integrating experimental and theoretical analyses *Am. J. Phys.* **78** 1120–7
[9] Kamela M 2007 An oscillating system with sliding friction *Phys. Teach.* **45** 110–3
[10] Millet P, Schreve J and Coxeter P 2006 Phase-space orbits and the ping-pong ball impact oscillator *Phys. Teach.* **44** 92–5
[11] Gluck P and Krakower Z 2010 A harmonic motion experiment *Phys. Educ.* **45** 611–6
[12] Marchewka A, Abbott D S and Beichner R J 2004 Oscillator damped by a constant-magnitude friction force *Am. J. Phys.* **72** 477–83
[13] Shaw D E 1979 Frictional force on rolling objects *Am. J. Phys.* **47** 887–8
[14] Hennekam W and Bontsema J 1991 Determination of F_r and K_d from the solution of the equation of motion of a cyclist *Eur. J. Phys.* **12** 59–63
[15] Farr J E 1983 Determining the air drag on a car *Phys. Teach.* **21** 320–1
[16] Hennekam W 1990 The speed of a cyclist *Phys. Educ.* **25** 141–6
[17] Andereck B S 1999 Measurement of air resistance on an air track *Am. J. Phys.* **67** 528–33

Carl Mungan is an Associate Professor of physics at the US Naval Academy, preparing 4000 officers for service in the American Navy and Marines. All students are required to take at least two semesters of physics as part of their preparation.